ORIGINAL RESEARCH

Synthesis, kinetic study and characterization of living anionic polymerized polystyrene in cyclohexane

Mohammad Reza Jozaghkar[1] · Farshid Ziaee[1] · SeyedMehrdad Jalilian[1]

Abstract

In this study, living anionic polymerization of styrene with varying molecular weights and narrow polydispersity index was successfully carried out at 45 °C in cyclohexane as a solvent and *sec*-butyllithium as an initiator. The kinetic study of the living anionic polymerization of styrene was investigated, as well as, the effect of its monomer concentration. For kinetic study, multi-stage dosing of initiator was proposed for calculation of the propagation rate constant and amounts of impurities. The results obtained by gel permeation chromatography (GPC) confirmed that polydispersity index of the synthesized polystyrene was close to the measured value. It has also revealed that the multi-stage dosing of initiator has been an appropriate and accurate method to determine the propagation rate constant. The results also demonstrated that the optimum initial concentration of the monomer in this system was 0.15 mol.L^{-1}. Tacticity and microstructure of the synthesized samples were studied by ^{13}C NMR technique. The probability of meso addition was calculated and the corresponding value was 0.395. ^{1}H NMR spectroscopy was used to obtain the number-average molecular weights of the samples, which were in accordance with the values estimated by GPC method. FTIR spectra showed that by detecting the changes in the areas ratio of two comparable bands at 1940 cm^{-1} and 1370 cm^{-1}, the molecular weights of the synthesized samples could be estimated. Thermal analysis indicated that very low molecular weight PS liquid resin has negative T_g and broad thermal decomposition range.

✉ Farshid Ziaee
f.ziaee@ippi.ac.ir

[1] Iran Polymer and Petrochemical Institute, P. O. Box: 14965/115, Tehran, Iran

Graphical abstract
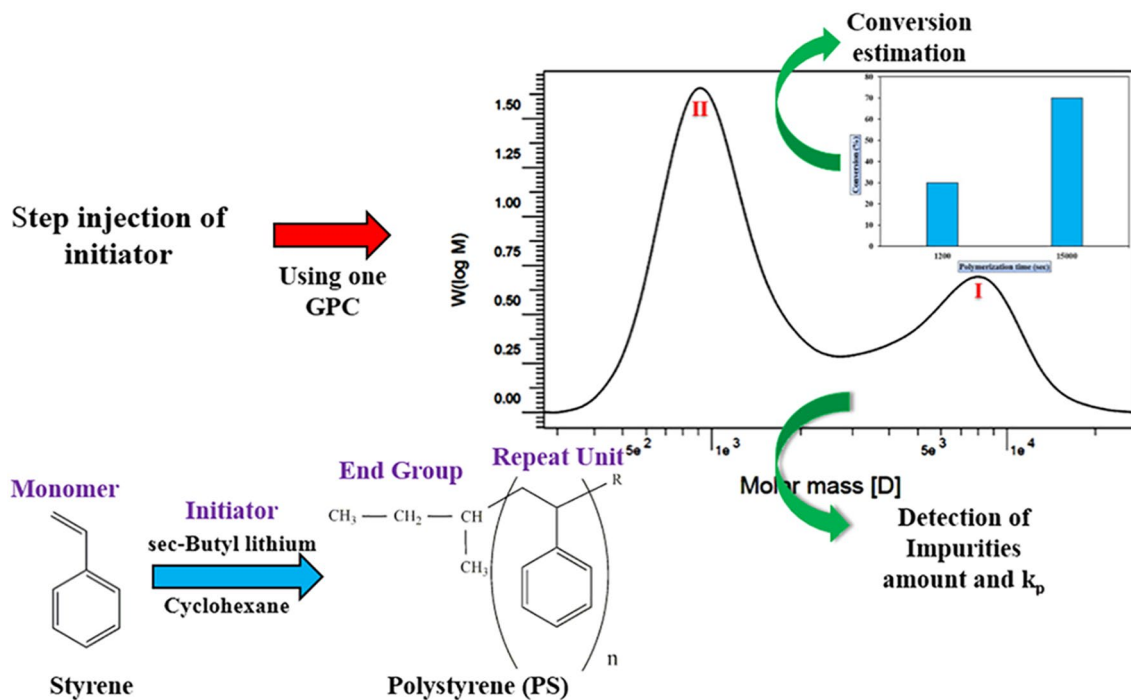
Keywords Living anionic polymerization · Polystyrene · Kinetic study · Monomer concentration · Characterization

Introduction

Living anionic polymerization has been used for decades to provide many valuable polymers with architectural precision, targetable molecular weights and narrow polydispersities at a modest polymerization temperature [1–3]. In addition, it is applicable to many monomers, especially nonpolar ones such as styrene and dienes which can stabilize a negative charge when accommodate into the active centers [4, 5].

Since, Szwarc and coworkers that first reported the living anionic polymerization of styrene in 1956, gradual improvements have been observed for synthesis of several chain-end functionalized polymers [6, 7]. The mechanism of the anionic polymerization of styrene with lithium as a counter ion in non-polar solvents has been well known [8] and comprehensive reviews have been published about the previous and current improvements in the living anionic polymerization using various initiating systems, as well [9, 10]. It has been proposed that trialkylaluminium and alkali metal hydrides are the well anionic initiators for controlling the styrene polymerization at elevated temperatures [11].

The understanding of polymerization kinetics and microstructure permits to tailor-made complex polymeric architectures, as well as, controlling time and rate of polymerization

(R_p) [12–14]. The researchers have been reported that counter ion, temperature and type of solvent significantly influenced the rates of initiation and propagation of polymerization [15, 16]. The study of anionic polymerization of styrene demonstrated that the activity of the anionic active site is intensely enhanced in polar solvents such as tetrahydrofuran (THF), because of the formation of loose ion pairs between the active sites and the counter ions. In this case, the polymerization was carried out at about − 78 °C. Otherwise, the polymerization could be completed in a few seconds. While, in non-polar solvents especially cyclohexane, due to the formation of tight ion pairs from the active sites and counter ions, the kinetic study of the polymerization was a straightforward than the polar one [17, 18].

Furthermore, it has been represented that dielectric constant and solvating power of solvent affected the rate of propagation and initiation in the anionic polymerization [19]. The solvent with relatively high dielectric constant and high solvating power produced polymers with high molecular weights due to the fact that R_p increased much more rapidly than R_i in the mentioned solvent. Johnson et al. [20] reported the kinetic study of anionic polymerization of butadiene and styrene. They found that kinetics of the polymerization initiation reaction of isoprene with butyllithium in cyclohexane varied significantly from that of the reaction of styrene and

butyllithium in benzene solution. The former demonstrated far more complex behavior than the latter. Lee and his coworkers [21] studied the molecular weight distribution of the living anionic polymerized species using the extraction of aliquots from the mixture at various reaction times. They precipitated the polystyrenes from each aliquot in a mixture of 2-propanol/methanol and analyzed by size exclusion chromatography (SEC) and temperature gradient interaction chromatography (TGIC) techniques.

This study was designed to estimate the kinetics parameters more easily using a gel permeation chromatography (GPC) pattern without the extraction of aliquots from the mixture during the polymerization reaction. For this purpose, a novel strategy (multi-stage dosing of initiator) was proposed. Additionally, the effect of monomer concentration was investigated on the molecular characteristics and GPC curves. Finally, the tacticity, molecular weight, microstructure and thermal behavior of the samples were investigated by ^{13}C nuclear magnetic resonance spectroscopy (^{13}C NMR), ^{1}H nuclear magnetic resonance spectroscopy (^{1}H NMR), Fourier-transform infrared spectroscopy (FTIR), thermogravimetric analysis (TGA) and differential scanning calorimetry (DSC), respectively.

Experimental

Materials

All chemicals and reagents including styrene monomer (99%), *n*-butyllithium (2.0 M in cyclohexane) and *sec*-butyllithium (1.4 M in cyclohexane) as initiators, 2-propanol (99.5%) as terminating agent, cyclohexane (99%), concentrated sulfuric acid (98%) and calcium hydride powder (95%) were supplied from Merck, Germany.

Living anionic polymerization

The living anionic polymerization of styrene was carried out under Ar atmosphere. At first styrene was purified with calcium hydride powder for several days to eliminate dissolved water. Then, purified styrene was distilled into a monomer buret by vacuum distillation at 50 mmHg and 60 °C. Second, cyclohexane was stirred over concentrated sulfuric acid for several weeks. After that, it was refluxed under inert atmosphere for a few hours and then injected into the glass-made container that was formerly transferred to the vacuum glove box. Then, the required amounts of *n*-butyllithium and monomer were injected into the glass-made container. The presence of colored solution confirmed the adequate purification of the system. Then, the solution in the glass-made container was transferred to the polymerization reactor. The reactor was immersed in the thermostatic

Table 1 Sample compositions for kinetic study of the living anionic polymerization of styrene in cyclohexane (200 mL) at 45 °C with initial monomer concentration of 0.15 mol.L^{-1}

Sample code	Peak number	Initiator amount (mL)	Polymerization time (min)	M_w ($\times 10^3$)	Đ
KPS1	I	1	20	7.98	1.11
	II	2	270	0.98	1.11
KPS2	I	0.5	20	18.70	1.0
	II	0.5	80	10.30	1.01
	III	0.5	170	4.48	1.02
	IV	0.5	270	2.65	1.12

Table 2 Effect of monomer concentration on the living anionic polymerization of styrene in cyclohexane (200 mL) at 45 °C, using 2.5 mL of initiator

Sample code	Monomer concentration (mol.L^{-1})	M_w ($\times 10^3$)	Đ
PS1	0.14	1.64	1.14
PS2	0.15	1.88	1.14
PS3	0.17	2.17	1.11
PS4	0.26	3.28	1.13
PS5	0.38	5.19	1.09
PS6	0.85	6.72	1.12

water bath (45 °C ± 0.1 °C) and under Ar atmosphere. The polymerization set up was designed according to design of Ndoni et al. [22].

For kinetic study, the desired amount of initiator was added into reaction vessel containing cyclohexane (200 mL) in the given time using a gastight syringe. The polymerization was initiated by adding purified monomer and terminated after 4.5 h using degassed 2-propanol (Table 1). The monomer conversion was estimated by gravimetric method. The samples designations and compositions for investigating the effect of monomer concentrations are summarized in Table 2. In these series of examinations, the initiator amount and polymerization temperature were kept constant and the solutions with different monomer concentrations were organized.

Characterization

GPC

Gel permeation chromatography (GPC) was performed in tetrahydrofuran (THF) at 1 mL.min^{-1} over an Agilent 1100 (USA) system equipped with differential refractometer detector and PLgel 5 μm OH-MIXED C 300 × 7.5 mm

(containing Agilent PS standard) at 30 °C. The concentration of solution was 1 g/L.

NMR

The solution samples for NMR spectra were scanned on a Bruker Avance 400 MHz (Germany) spectrometer. Sample concentration was about 20% (w/v) for ^{13}C NMR and 5% (w/v) for ^1H NMR using a 5 mm NMR tube at 20 °C. ^1H NMR spectra were scanned over 32 K data points, spectral width 16 ppm, acquisition time 1.59 s, relaxation delay 10 s, pulse width 30° and 4 scans. ^{13}C NMR spectra were scanned over 64 K data points, spectral width 220 ppm, acquisition time 1.59 s, relaxation delay 2 s, pulse width 90° and 20,000 scans.

FTIR

Identification of the synthesized samples was also carried out by a FTIR Bruker-IFS48 (Germany) spectrometer in the wavenumber range of 4000–400 cm^{-1}.

Thermal analysis

Thermogravimetric analysis (TGA) was performed using a TGA laboratory instrument (Toledo, Switzerland) from 25 to 600 °C under nitrogen purge at a heating rate of 10 °C/min. The DSC (Toledo, Switzerland) measurement was carried out at the heating rate of 10 °C min^{-1} under nitrogen atmosphere.

Results and discussion

It is well known that reagent purification is crucial for anionic polymerization because the deactivation of the initiator is depending on the presence of impurities (moisture, oxygen, etc.) in the system [23, 24]. The presence of impurity and its effect on the molecular weight and rate of polymerization can be elucidated from GPC distribution plot. In this study, the multi-stage dosing of initiator was used for the estimation of k_p (propagation rate constant) and amounts of impurities at the beginning of the polymerization reaction. As was mentioned, cyclohexane is an excellent solvent for this purpose, because of the formation of tight ion pairs among the active sites and counter ions which were contributed to the stability of the anionic system [25].

GPC pattern of KPS1 with a two-stage dosing is shown in Fig. 1. Polymer conversion versus polymerization time is presented in the inset diagram, as well. The results showed that the polydispersity indexes ($Đ$) of both peaks were close to their true values. However, the intensity of peak I (appearing at higher molecular weight region) was markedly lower than that of the peak II. It was shown that conversion for step I was 30%, too. Because the anionic polymerization initiator was entirely dissociated before the polymerization was started, the simple classic kinetics could be used for the estimation of k_p and amounts of impurities in the system [26]. The k_p was defined by the integration of the first-order rate equation as follow:

$$[M] = [M]_0 e^{-k_p[I]_0 t}, \tag{1}$$

where, $[M]$, $[M]_0$ and $[I]_0$ are concentrations of monomer at time t, the initial concentration of the monomer and the total

Fig. 1 GPC chromatogram of KPS1 in cyclohexane (200 mL) at 45 °C (Inset: conversion as a function of polymerization time)
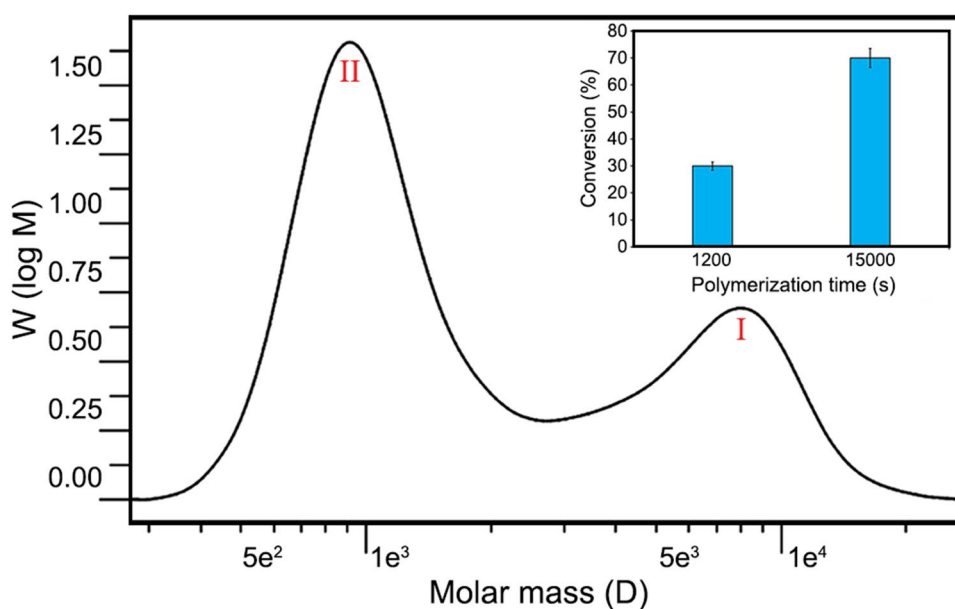
concentration of the initiator before dissociation, respectively. In the anionic polymerization because the number of the formed molecules is equal to the number of chain centers, the degree of polymerization can be defined by Eq. (2):

$$X_n = \frac{[M]_0 - [M]}{[I]_0}. \tag{2}$$

In practice, trace amounts of impurities can react with initiator and decline its concentration for polymerization reaction. Thus, it is necessary to make simple modification for Eq. (2) as follows:

$$X_n = \frac{[M]_0 - [M]}{[I]_{0p}}, \tag{3}$$

where $[I]_{0p}$ is the concentration of the pure initiator which can be participated in the polymerization reaction as given by the following equation:

$$[I]_0 = [I]_{0p} + [I]_{0i}, \tag{4}$$

where $[I]_{0i}$ is the initiator concentration which reacts with impurities.

For anionic polymerization with a two-stage dosing, X_n could be defined as follows:

$$X_{n1} = \frac{[M]_0 - [M]_1}{[I]_{0p}} + \frac{[M]_1 - [M]_2}{[I]_{0p} + [I]_1}, \tag{5}$$

$$X_{n2} = \frac{[M]_1 - [M]_2}{[I]_{0p} + [I]_1} = \frac{[M]_1}{[I]_{0p} + [I]_1}, \tag{6}$$

where X_{n1} and X_{n2} denote the number-average degree of polymerization values for peaks I and II, respectively. $[M]_1$ is the residual monomer concentration before the 2nd-stage of dosing, $[I]_1$ is initiator concentration in the second stage of dosing and $[M]_2$ is the residual monomer at the end of the polymerization reaction. It should be mentioned that the two terms on the right-hand side of Eq. (5) represent the degree of polymerization for the first and second stages of dosing, respectively. The right-hand side term of Eq. (6) demonstrates degree of polymerization for second stage of dosing.

According to gravimetric method, it was found that monomer conversion was 100% and $[M]_2$ was equal to zero. To ensure the results of the gravimetric method, another initiator injection was performed after 4.5 h for another sample with similar experimental condition. The GPC spectrum of both samples was the same, which confirmed the gravimetric results.

Using X_{n1} and X_{n2} values obtained from GPC distribution plot, $[I]_{0p}$ could be calculated by simultaneous solving of the Eqs. (5) and (6). Subsequently, by replacing the obtained parameters to the Eq. (1), k_p could be obtained (0.67 L.mol^{-1}.s^{-1}). The k_p obtained in this study using multi-stage dosing of initiator, was very close to data of the Lee et al. [21] and was in good agreement with the classical kinetic theory in anionic polymerization.

To calculate the average of k_p, more accurately, a four-stage dosing of initiator was used. Figure 2 represents GPC graph of the sample KPS2. Similar to KPS1, peak I in the GPC pattern of KPS2 showed lower intensity than peaks II and III, indicating the reaction of impurities with initiator at the beginning of the polymerization. The conversion versus polymerization time for KPS2 is shown in the inset diagram in Fig. 2, showing that the conversion at stage 1 was only

Fig. 2 GPC chromatogram of KPS2 in cyclohexane (200 mL) at 45 °C (Inset: conversion as a function of polymerization time)
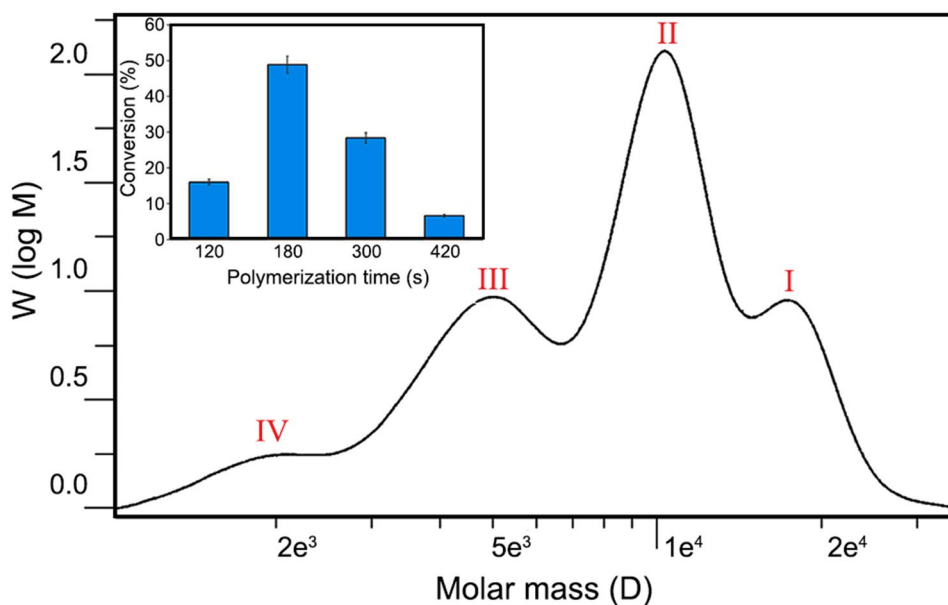
about 16%. For calculation of $[I]_{0p}$ and k_p, simultaneous solving of the following four equations was needed:

$$X_{n1} = \frac{[M]_0 - [M]_1}{[I]_{0p}} + \frac{[M]_1 - [M]_2}{[I]_{0p} + [I]_1}$$
$$+ \frac{[M]_2 - [M]_3}{[I]_{0p} + [I]_1 + [I]_2} + \frac{[M]_3}{[I]_{0p} + [I]_1 + [I]_2 + [I]_3}, \quad (7)$$

$$X_{n2} = \frac{[M]_1 - [M]_2}{[I]_{0p} + [I]_1} + \frac{[M]_2 - [M]_3}{[I]_{0p} + [I]_1 + [I]_2} + \frac{[M]_3}{[I]_{0p} + [I]_1 + [I]_2 + [I]_3}, \quad (8)$$

$$X_{n3} = \frac{[M]_2 - [M]_3}{[I]_{0p} + [I]_1 + [I]_2} + \frac{[M]_3}{[I]_{0p} + [I]_1 + [I]_2 + [I]_3}, \quad (9)$$

$$X_{n4} = \frac{[M]_3 - [M]_4}{[I]_{0p} + [I]_1 + [I]_2 + [I]_3}. \quad (10)$$

where X_{n1}, X_{n2}, X_{n3} and X_{n4} denote the number-average degree of polymerization values for peaks I, II, III and IV, respectively. The values of $[M]_2$ and $[M]_3$ are the residual monomer concentrations before third and fourth stages of dosing, respectively, and those of $[I]_2$ and $[I]_3$ are initiator concentrations in the third and fourth stages of dosing, respectively, and $[M]_4$ is the residual monomer at the end of polymerization reaction. According the gravimetric method, it was revealed that monomer conversion was 100% and $[M]_4$ was equal to zero.

Using these equations, k_p value was estimated to be 0.65 L.mol^{-1}.s^{-1}. Interestingly, there is a satisfactory agreement between k_p obtained by the two-stage and four-stage dosings. This is particularly important in the case of the mixture of polar and non-polar solvents. In fact, in the presence of polar solvents, the rate of polymerization reaction was dramatically increased [25]. Thereupon, in these systems, the high number of initiator dosing resulted in the peaks overlap and reduced the measurement accuracy of the propagation rate constant. For these systems, the two-stage dosing of initiator was more appropriate.

Effects of monomer concentration on the molecular characteristics and GPC curves are showed in Fig. 3. The symmetrical GPC curve and the low Đ demonstrated the great-controlled characteristics of the samples PS1 and PS2 with initial monomer concentrations of 0.14 and 0.15 mol. L^{-1}, respectively (Figs. 3a, b). However, a further increase in the initial monomer concentration (i.e., 0.17 and 0.26 mol. L^{-1} for PS3 and PS4, respectively) led to appearance of a small second peak on the right-hand side of the GPC graphs. A distinct second peak was appeared at higher molecular weights for PS5 and PS6 (Figs. 3c–f). It can be concluded that for well-controlled characteristics of polystyrene in the aforementioned system, the optimum amount of initial concentration of the styrene should not exceed 0.15 mol.L^{-1}.

It has been reported that one of the consequential parameters on the stereochemistry of styrene polymerization is the monomer concentration [27]. According to Hatada et al. [28] and Muller et al. [29] a great quantity of initial concentration of the monomer may alter the characteristics of the medium and mechanism of polymerization.

^{13}C NMR

To have knowledge of polymer chain architecture, it is necessary to acquire information about the relation between structure and features [30]. Principally, due to higher resolution and more extensive sweep width, ^{13}C NMR is used for tacticity determination of the polymers.

Figure 4 shows the solution state ^{13}C NMR spectrum of PS in chloroform-d. In addition, the expanded ^{13}C NMR of quaternary aromatic and methylene carbons, are showed in the insets diagrams. As can be seen in Fig. 4, peak of this quaternary aromatic carbon has been split into 10 peaks. Thus, in statistical analysis, it has pentad sequence-distributions where left section is rich in meso sequences and the right section is rich in racemic ones. On the other hand, the peaks with assignment numbers of 1, 2 and 3 are syndiotactic, with those denoted with the numbers of 4, 5, 6 and 7 are atactic and with those designated with 8, 9 and 10 are isotactic [31]. The experimental results were evaluated for Bernoullian and first-order Markov statistical models of chain propagation and results are presented in Table 3 [30]. The assignments were confirmed by the results of Pedroza and Tavares work [32].

In statistical assessment, the probability of meso (P_m) and racemic (P_r) sequences are expressed by Eqns. (11) and (12), respectively. The rr, mr and mm triad sequences have syndiotactic, atactic and isotactic parts of chain, respectively [33].

$$P_m = (2mm + mr)/2, \quad (11)$$

$$P_r = 1 - P_m = (2rr + mr)/2. \quad (12)$$

It should be noted that the relationship between pentad and triad sequences were attained using Eqns. (13–15) which finally enabled the calculation of P_m value.

$$mm = mmmm + mmmr + rmmr \quad (13)$$

$$mr = mmrm + mmrr + rmrm + rmrr \quad (14)$$

$$rr = mrrm + mrrr + rrrr \quad (15)$$

Using Eqns. (11–15) and integrating sequences area in Fig. 4, the calculated value of P_m for all samples was equal to 0.395. This indicated that the racemic addition was higher
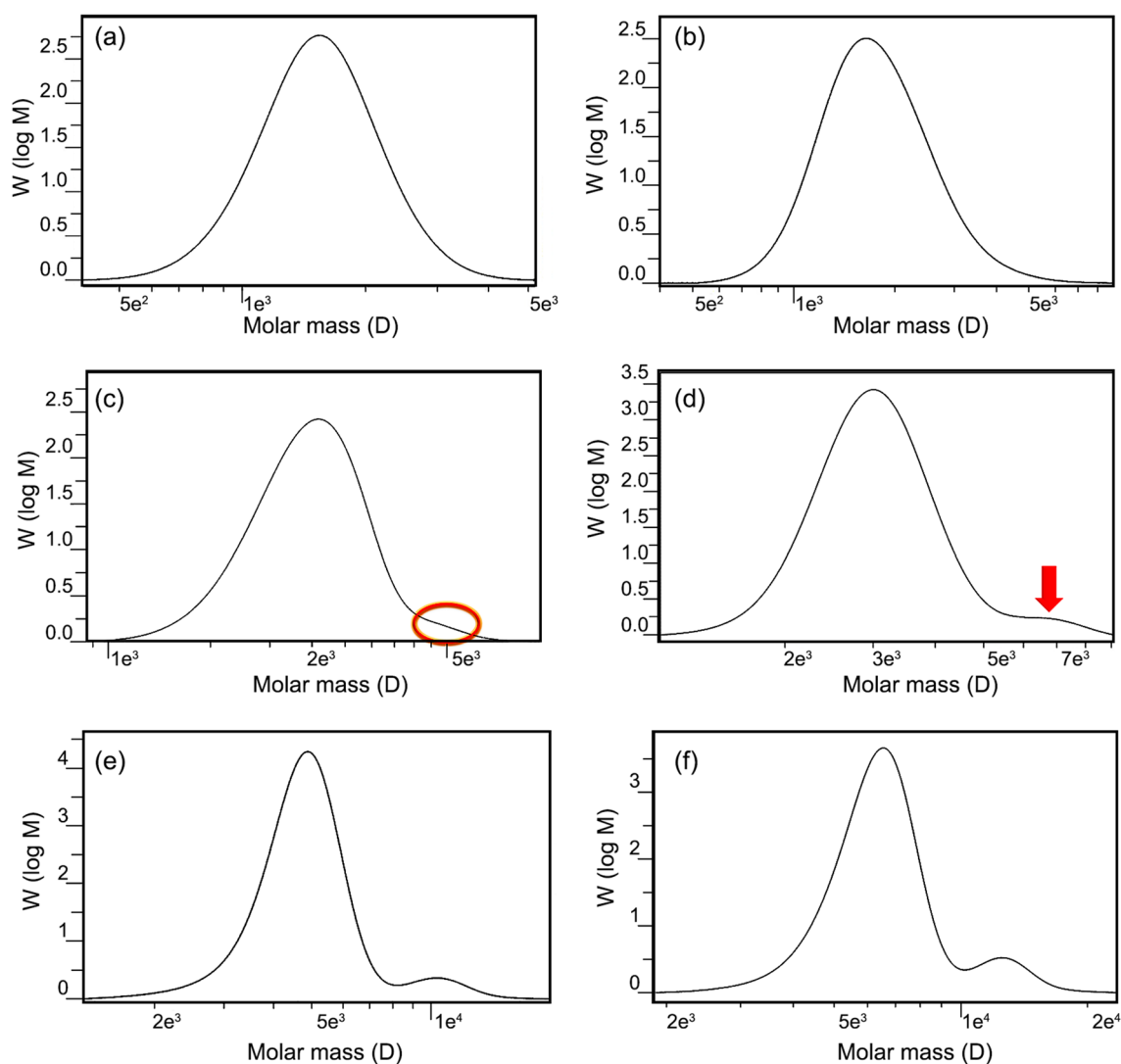
Fig. 3 GPC chromatograms of PS samples at various monomer concentrations but constant amount of initiator and temperature: **a** PS1, **b** PS2, **c** PS3, **d** PS4, **e** PS5 and **f** PS6

than the meso one. Moreover, our synthesized polystyrene has several deviations from the ideal random case ($P_m = 0.5$). This can be attributed to the bulky nature of the benzene ring in the PS monomer [31]. It is challenging to compare these results with those reported in the research work that synthesized PS via radical polymerizations at 50 °C, 150 °C and 250 °C, and their P_m values were 0.378, 0.398 and 0.402, respectively [31]. These findings confirmed that the polystyrene with $P_m = 0.39$ could be synthesized by living anionic polymerization at a temperature much lower than that of the radical polymerization.

Relative to the quaternary aromatic carbon, the methylene carbon of polystyrene main chain is perceived at upper magnetization field. It can be observed in Fig. 4 that peak of this carbon has been split into about 8 peaks in chemical shift rang of about 6.5 ppm. Thereupon, statistically,

it has hexad sequence-distributions where right section is rich in racemic sequences and the left section is rich in meso ones. The assignment of peaks detected in Fig. 4 was accomplished according to Kawamura's assignment [34] on the hexad sequences of PS methylene carbon. The experimental data were tested for Bernoullian and first-order Markovian models and the results are demonstrated in Table 4. The sum of squared differences between observed and calculated data was also used for the comparison of these two statistical models. These data are also shown in Tables 3 and 4, respectively. Based on the results of these Tables, 1st-order Markovian model fits slightly better than the experimental consequences. However, presence of some deviations might be affiliated to the defective assignment of the peaks.
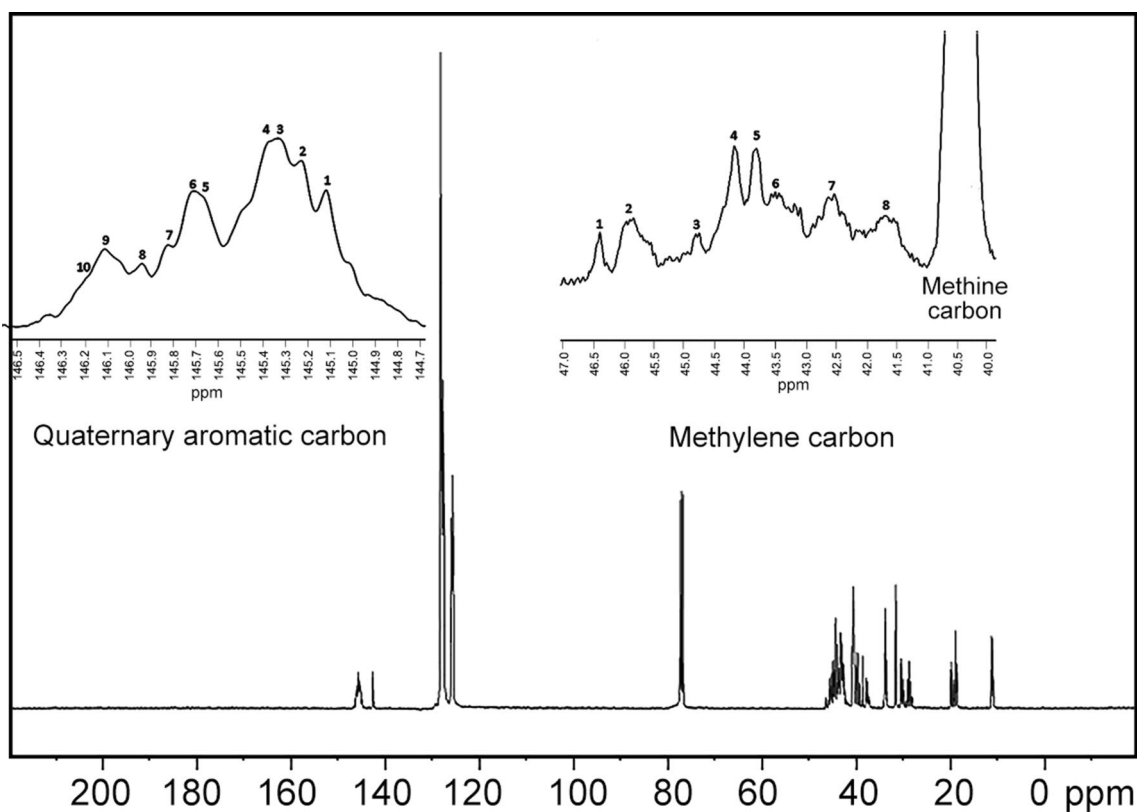
Fig. 4 ^{13}C NMR spectrum of PS in CDCl$_3$ at 20 °C (Insets: expanded ^{13}C NMR peaks of quaternary aromatic and methylene carbons)

Table 3 Normalized pentad sequences of quaternary aromatic carbon and its calculated Bernoullian and first-order Markov statistics in CDCl$_3$ at 20 °C

Peak no.	Pentad micro-structure	Chemical shift (ppm)	Observed	Bernoullian calculation[a]	First-order Markov calculation[b]
1	rrrr	145.305	0.1195	0.1336	0.1254
2	mrrr	145.415	0.1143	0.1747	0.1723
3	mrrm	145.524	0.1364	0.0571	0.0603
4	rmrr	145.550	0.2196	0.1743	0.1844
5	rmrm	145.836	0.0887	0.1563	0.1488
6	mmrr	145.902	0.1089	0.1563	0.1510
7	mmrm	146.018	0.0573	0.0374	0.0364
8	rmmr	146.120	0.0453	0.0481	0.0462
9	mmmr	146.287	0.1128	0.0374	0.0458
10	mmmm	146.301		0.0244	0.0294

[a]Sum square difference: 2.08×10^{-3}

[b]Sum square difference: 1.71×10^{-3}

^{1}H NMR

The diversity in the chemical shifts between the chain ends and the main chain repeating units agreed with the number-average molecular weight (M_n) calculations by the end-group assessment technique. ^{1}H NMR, as a quantitative method that requires no calibration, is a simple and relatively precise method to determine the molecular weight of polymers. For the determination of M_n using ^{1}H NMR, prominently, the measured values are succeeding the data from other suggested techniques [35, 36]. ^{1}H NMR spectra of very low molecular weight PS ($M_{n\ GPC} = 513$ g.mol^{-1}) and medium molecular weight PS ($M_{n\ GPC} = 4600$ g.mol^{-1}) resins are depicted in Fig. 5(A, B), respectively, with corresponding

Table 4 Normalized hexad sequences of the methylene carbon and its calculated Bernoullian and first-order Markov statistics in CDCl$_3$ at 20 °C

Peak no.	Pentad microstructure	Chemical shift (ppm)	Observed	Bernoullian calculation[a]	1st -order Markov calculation[b]
1	mrmrm	46.419	0.0293	0.0289	0.0372
2	mrmrr + mrrrm + rrmrr	45.922	0.1088	0.1388	0.1376
3	mrrrr	44.782	0.0748	0.1141	0.1083
4	mmmrm + rmmrm + rrrrr	44.204	0.1688	0.1742	0.1678
5	mmmrr + rmmrr	43.841	0.1330	0.1056	0.105
6	rmrrr + mmrrr + rmmmr	43.532	0.1670	0.1991	0.1985
7	mmrrm + rmrrm + mmmmr + mmmmm	42.558	0.1709	0.1503	0.1498
8	mmrmm + mmrmr + rmrmr	41.737	0.1474	0.089	0.0958

[a]Sum square difference: 1.44×10^{-1}

[b]Sum square difference: 1.42×10^{-1}

peaks assigned according to the spectra of standard PS. The peak observed in the range of 0.7–0.9 ppm is related to methyl group's protons which are assigned with "a" in Fig. 5. The peak in the range of 6.2–7.3 ppm is related to aromatic protons which are assigned with "b". It is noteworthy that the absence of three peaks of doublet of doublet in the chemical range of 4–6 ppm confirmed that there was no unreacted monomer in the system.

The peaks distinguished with "c" are attributed to aliphatic methine and methylene groups' protons. The number of repeating units (n) of the polystyrene can be determined by comparing the relative intensity of peak of aromatic protons to that of the methyl group [37]:

$$n = \{(b/5)/(a/6)\} \tag{16}$$

Thus, M_n can be estimated by substituting Eq. (16) for n in Eq. (17):

$$M_n = nM_{0s} + M_i, \tag{17}$$

where M_{0s} is the molecular weight of styrene repeating unit, and M_i is the molecular weight of the end groups (alkyl lithium of initiator). The calculated M_n using ^{1}H NMR for very low molecular weight PS and medium molecular weight PS samples were 450 and 4700 g.mol^{-1}, respectively, which was in good agreement with the GPC results. The consistency of data affirmed good reliability of our quantitative NMR analysis. However, a small deviation between ^{1}H NMR and GPC results were due to overlapping of CDCl$_3$ and aromatic protons peaks. It is crucial to note that calculation of M_n using ^{1}H NMR spectroscopy is accurate only for low molecular weight polymers. This is due to the decrease in accuracy of integration of high molecular weight polymers and the inability to detect the end groups [38].

FTIR

It has been known that FTIR spectroscopy is one of the simplest, robust and powerful characterization's techniques to elucidate the structure and composition of the polymers. The wavenumber in the IR region is proportional to the material content according to Beer–Lambert law [39]. There are several successful studies in this area. Zhang et al. [40] used FTIR spectra for quantification of bound styrene in SBR, SBS and SIS copolymers. Deygen and his coworkers [41] determined PEGylated conjugate composition using FTIR. Bakhshi and coworkers [42] investigated the composition of poly(butyl acrylate-*co*-glycidyl methacrylate) using FTIR and compared with ^{1}H NMR data. Figure 6 depicts FTIR spectra of four PS samples with different molecular weights. The peaks appeared in the region 3150–3050 cm^{-1} are related to the aromatic C–H stretching vibration absorptions. While, peaks in the region 3000–2850 cm^{-1} are corresponded to asymmetric and symmetric stretching vibrations of methylene group –CH$_2$, respectively. The weak combination and overtone absorptions are appeared in 2000–1665 cm^{-1} range. The absorption peaks at wavenumbers of about 1630, 990, and 910 cm^{-1} may be corresponded to the same new combination for low molecular weight polystyrene. The absorption peak at the wavenumber of 1370 cm^{-1} is corresponded to methyl C-H of initiator. The characteristic absorption peaks at the wavenumbers of 756 cm^{-1} and 698 cm^{-1} are attributed to C-H out-of-plane bending absorptions.

For preparing the calibration curve, it was postulated that polystyrene was composed of two different units (styrene units and alkyl groups of the initiator units). According to Beer–Lambert law, plot of absorbance against concentration should be linear. To analyze the sample with an unknown composition, the appropriate bands of a known sample should be selected and calibration curve should be plotted using the absorbance values at these wavenumbers.

Fig. 5 ^{1}H NMR spectra of PS samples with different M_n values for: **A** very low molecular weight PS resin with $M_{nGPC} = 430$ g.mol^{-1} and **B** medium molecular weight PS resin with $M_{nGPC} = 4600$ g. mol^{-1}
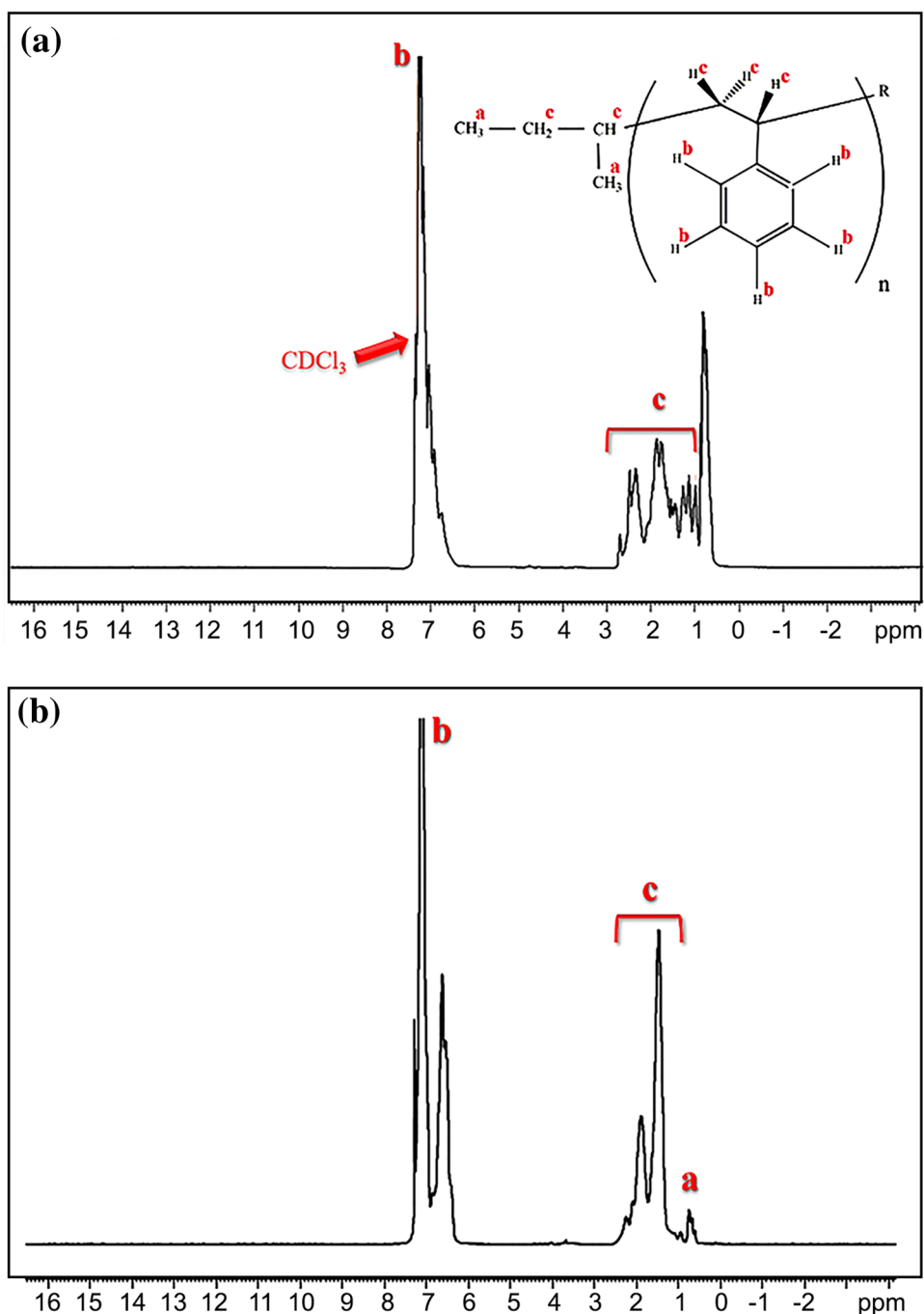

Therefore, in the case of polystyrene containing alkyl end groups, the ratio of the overtone and combination absorption of mono-substituted aromatic rings of styrene (1940 cm^{-1}) to that of the absorbance of asymmetric bending mode of methyl C-H of initiator (1370 cm^{-1}) was used for calibration. This relation was linear and could be denoted by Eq. (18) obtained from a linear fit of the FTIR data.

$$Y = 0/0118X - 0/7302,$$ (18)

where Y is the absorbance ratio of A_{1940}/A_{1370} and X is styrene molar concentration (%) which was obtained from GPC results. The molecular weight can be estimated by the following equation:

$$M_n = \frac{X}{100 - X} \times M_{0s} + M_i.$$ (19)

Fig. 6 FTIR spectra of PS samples with different molecular weights
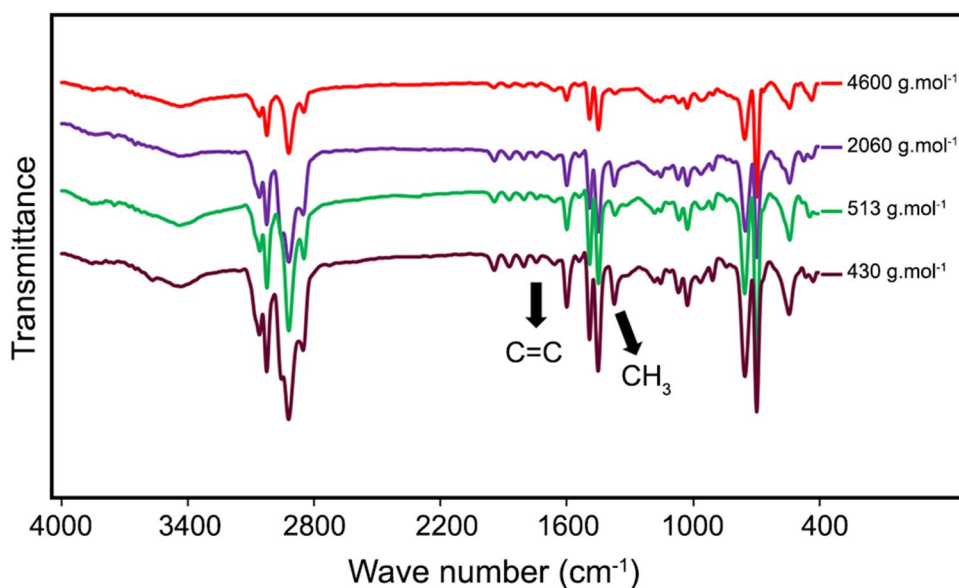
Thermal behavior

The molecular weight is one of the important structure factors that significantly impacts on the physical properties of PS. The effect of molecular weight on the thermal stability of the synthesized samples is depicted in Fig. 7. As it can be seen that the initial degradation of PS with $M_n = 430$ g.mol^{-1} was started at about 100 °C, while PS with $M_n = 4600$ g.mol^{-1} was started to degrade at about 340 °C. Also, a broad and pronounced multi-stage degradation curve can be seen for very low molecular weight resin. The pronounced multi-stage degradation pattern in very low molecular weight sample might be attributed

to the more significant influence of the repeating units. About 25% weight loss at each stage demonstrated the depolymerization of the repeating unit for this sample. The increase in molecular weight leads to a restriction of polymer mobility and an increase in degradation temperature, suggesting more thermal stability [43].

It is worth noting that glass transition temperature (T_g) is predominantly dependent on molecular weight, especially when the degree of polymerization is low. DSC curves for atactic-PS of different molecular weights are shown in Fig. 8a. It could be observed that as the molecular weight of PS increased, the T_g shifted to higher value. The results also showed that as molecular weight

Fig. 7 TGA curves for degradation of PS samples (dotted lines are DTG curves)
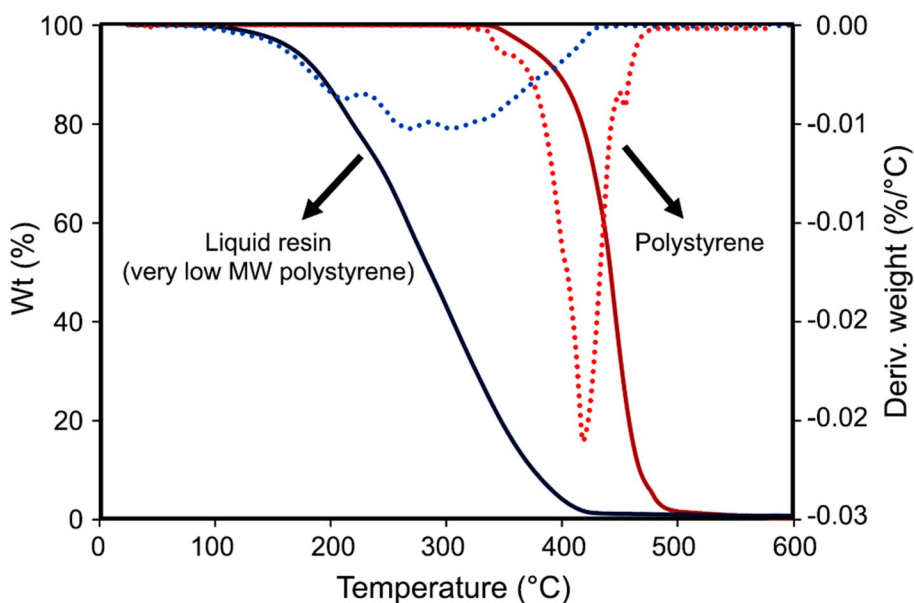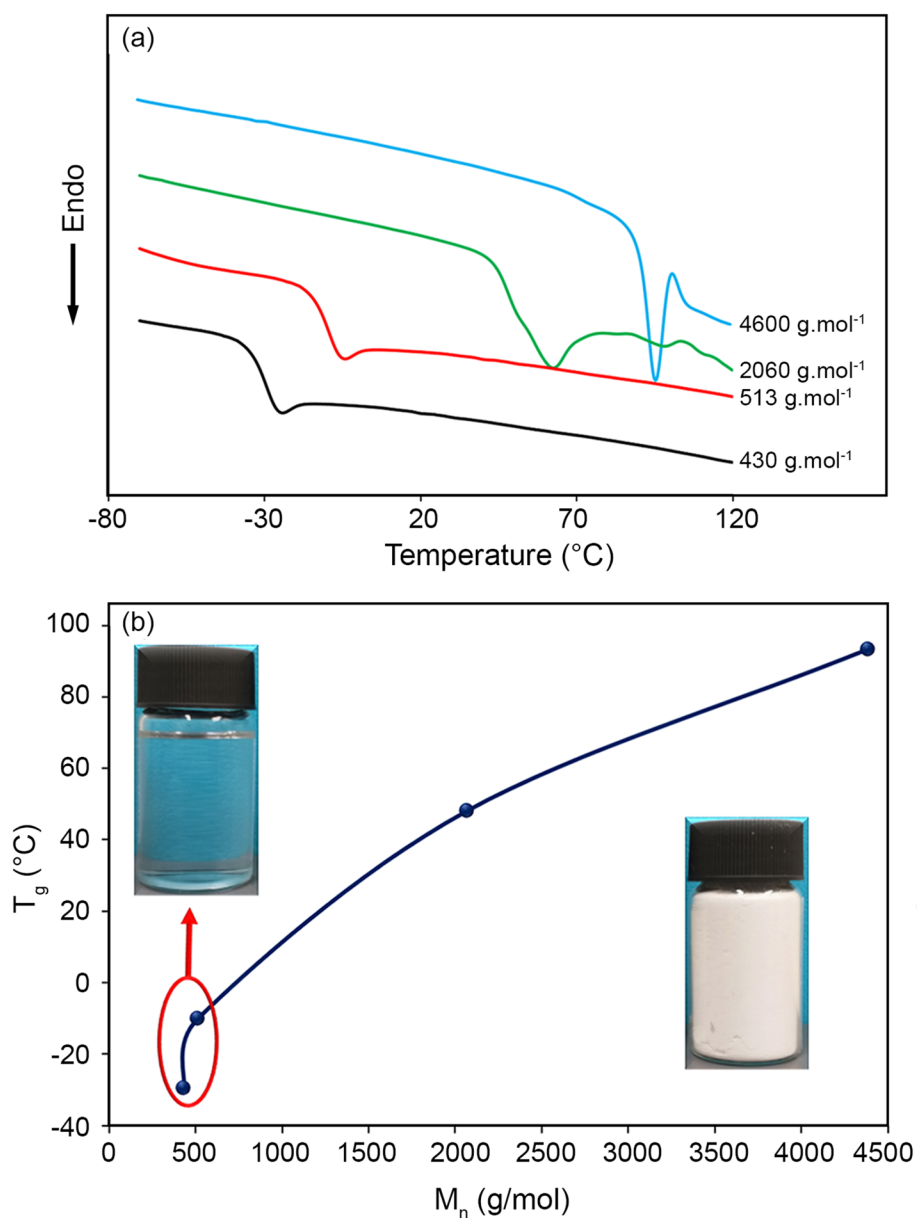
Fig. 8 a DSC thermograms for PS samples with different molecular weights and **b** Plot of T_g as a function of M_n values for PS samples with different molecular weights

increased, T_g value increased rapidly at first and then elevated more slowly (Fig. 8b).

Conclusion

In this work, polystyrene with various molecular weights and narrow molecular weight distribution was synthesized via living anionic polymerization. The kinetic study, investigation of the monomer concentration effect on the GPC graph and characterization of the synthesized PS led to the following deductions:

1. The multi-stage dosing of initiator is a useful and straightforward method for estimation of the propagation

rate constant and amounts of impurities in the system using GPC pattern. Decrement of the first peak of the GPC graph revealed that a small amount of initiator was reacted with impurities. Also, the results showed that the propagation rate constant (k_p) for the living anionic polymerization of styrene with *sec*-butyllithiumin in cyclohexane medium at 45 °C was about 0.65 L.mol^{-1}. s^{-1}.

2. Based on the observed GPC graphs, it was found that in this system, optimum initial concentration of the monomer was 0.15 mol.L^{-1} and further increasing was led to appearance of the second peak at the higher molecular weight region.

3. Using ^{13}C NMR method, assignment of all stereosequences was achieved on quaternary aromatic carbon

at pentad level and methylene carbon at hexad level. Observed data were compared with Bernoullian and first-order Markov statistics. The results showed that experimental data was fitted moderately better with first-order Markov propagation model. Moreover, polystyrene with $P_m = 0.39$ could be obtained via living anionic polymerization at a temperature much lower than the radical polymerization.

4. ^{1}H NMR method was used to further characterize the PS samples and estimate of the M_n values. The consistence of data with GPC results confirmed good reliability of our quantitative NMR analysis.

5. FTIR spectral data was used to study bands intensity as a function of polymer composition. The clear slope change was observed for absorbance band area ratio of A_{1940}/A_{1370} vs. molar concentration.

6. The DSC and TGA results demonstrated that the very low molecular weight PS liquid resins had glass transition temperature lower than 0 °C and showed lower degradation temperature but broader curve. Also, multistage degradation was more pronounced in the very low molecular weight PS resin.

References

1. Glatzel J, Noack S, Schanzenbach D, Schlaad H (2021) Anionic polymerization of dienes in 'green'solvents. Polym Int 70(2):181–184
2. Wang J, Cao M, Zhou P, Wang G (2020) Exploration of a living anionic polymerization mechanism into polymerization-induced self-assembly and site-specific stabilization of the formed nano-objects. Macromolecules 53(8):3157–3165
3. Goseki R, Koizumi T, Kurakake R, Uchida S, Ishizone T (2021) Living anionic polymerization of 4-halostyrenes. Macromolecules 54(3):1489–1498
4. Vijayaraghavan R, Pringle JM, MacFarlane DR (2008) Anionic polymerization of styrene in ionic liquids. Eur Polym J 44(6):1758–1762
5. Liu P, Ma H, Huang W, Shen H, Wu L, Li Y, Wang Y (2016) The determination of sequence distribution in the living anionic copolymerization of styrene and strong electron-donating DPE derivative-1, 1-bis (4-N, N-dimethylanimophenyl) ethylene. Polymer 97:167–173
6. Szwarc M (1998) Living polymers. Their discovery, characterization, and properties. J Polym Sci A1 36(1):9–13
7. Hirao A, Matsuo Y, Goseki R (2019) Synthesis of novel block polymers with unusual block sequences by methodology combining living anionic polymerization and designed linking chemistry. J Polym Res 26(12):1–20
8. Morita H, Van Beylen M (2019) The Mechanism of the propagation in the anionic polymerization of polystyryllithium in nonpolar solvents elucidated by density functional theory calculations. A study of the negligible part played by dimeric ion-pairs under usual polymerization conditions. Polymers 11(6):1022
9. Hirao A, Goseki R, Ishizone T (2014) Advances in living anionic polymerization: from functional monomers, polymerization systems, to macromolecular architectures. Macromolecules 47(6):1883–1905
10. Ito S, Goseki R, Ishizone T, Hirao A (2014) Synthesis of well-controlled graft polymers by living anionic polymerization towards exact graft polymers. Polym Chem 5(19):5523–5534
11. Carlotti S, Menoret S, Desbois P, Nissner N, Warzelhan V, Deffieux A (2006) Sodium hydride/trialkylaluminum complexes for the controlled anionic polymerization of styrene at high temperature. Macromol Rapid Comm 27(12):905–909
12. Ziaee F, Ronagh-Baghbani M, Jozaghkar MR (2020) Microstructure characterization of low molecular weight polybutadiene using the chain end groups by nuclear magnetic resonance spectroscopy. Polym Bull 77(5):2345–2365
13. Tsagkalias IS, Loukidi A, Chatzimichailidou S, Salmas CE, Giannakas AE, Achilias DS (2021) Effect of Na-and organomodified montmorillonite/essential oil nanohybrids on the kinetics of the in situ radical polymerization of styrene. Nanomaterials 11(2):474
14. Punyodom W, Limwanich W, Meepowpan P, Thapsukhon B (2021) Ring-opening polymerization of ε-caprolactone initiated by tin (II) octoate/n-hexanol: DSC isoconversional kinetics analysis and polymer synthesis. Des Monomers Polym 24(1):89–97
15. Mark JE, Erman B, Roland M (2013) The science and technology of rubber. Academic Press, Massachusetts
16. McGrath JE, Hickner MA, Höfer R (2013) Polymers for a sustainable environment and green energy. Polym Sci 10:849
17. Takahashi Y, Nagaki A (2019) Anionic polymerization using flow microreactors. Molecules 24(8):1532
18. Li Z, Chen J, Su L, Zou B, Zhan P, Guan Y, Zheng A (2017) A controlled synthesis method of polystyrene-b-polyisoprene-b-poly (methyl methacrylate) copolymer via anionic polymerization with trace amounts of THF having potential of a commercial scale. RSC Adv 7(16):9933–9940
19. Weideman I, Pfukwa R, Klumperman B (2017) Phosphazene base promoted anionic polymerization of n-butyraldehyde. Eur Polym J 93:97–102
20. Johnson AF, Worsfold DJ (1965) Anionic polymerization of butadiene and styrene. J Polym Sci A1 3(2):449–455
21. Lee W, Lee H, Cha J, Chang T, Hanley KJ, Lodge TP (2000) Molecular weight distribution of polystyrene made by anionic polymerization. Macromolecules 33(14):5111–5115
22. Ndoni S, Papadakis CM, Bates FS, Almdal K (1995) Laboratory-scale setup for anionic polymerization under inert atmosphere. Rev Sci Instrum 66(2):1090–1095
23. Ma Q, Leng X, Han L, Liu P, Li C, Zhang S, Lei L, Ma H, Li Y (2020) Regulation of cis and trans microstructures of isoprene units in alternating copolymers via "space-limited" living species in anionic polymerization. Polym Chem 11(15):2708–2714
24. Yang L, Shen H, Han L, Ma H, Li C, Lei L, Zhang S, Liu P, Li Y (2020) Sequence regulation in living anionic terpolymerization of styrene and two categories of 1, 1-diphenylethylene (DPE) derivatives. Polym Chem 11(32):5163–5172
25. Hadjichristidis N, Hirao A (2015) Anionic polymerization: principles, practice, strength, consequences and applications. Springer, Berlin
26. Chanda M (2013) Introduction to polymer science and chemistry. CRC Press, Florida
27. Noh SK, Kim S, Yang Y, Lyoo WS, Lee DH (2004) Preparation of syndiotactic polystyrene using the doubly bridged dinuclear titanocenes. Eur Polym J 40(2):227–235
28. Tanaka Y, Sato H (1976) Sequence distribution of cis-1, 4-and trans-1, 4-units in polyisoprenes. Rubber Chem Technol 49(5):1269–1275
29. Hatada K, Ute K, Tanaka K, Okamoto Y, Kitayama T (1986) Living and highly isotactic polymerization of methyl methacrylate by t-C 4 H 9 MgBr in toluene. Polym J 18(12):1037

30. Jozaghkar MR, Ziaee F, Azar AS (2020) Investigation of poly (α-methyl styrene) tacticity synthesized by photo-polymerization. Polym Bull 78:5303–5314

31. Ziaee F, Nekoomanesh M, Mobarakeh HS, Arabi H (2008) The effect of temperature on tacticity for bulk thermal polymerization of styrene. E-Polymers 8(1):41

32. Pedroza OJO, Tavares MIB (2005) The influence of physical treatment in the polystyrene pentads microstructure determination by NMR. Polym Test 24(5):604–606

33. Zohuri G, (2012) Polymer science: a comprehensive reference, Science direct, ISBN 978-0-08-087862-1.

34. Kawamura T, Toshima N, Matsuzaki K (1994) Comparison of ^{13}C NMR spectra of polystyrenes having various tacticities and assignment of the spectra. Macromol Rapid Comm 15(6):479–486

35. Chen DX, Gao LF, Li XH, Tu YF (2017) Precise molecular weight determination and structure characterization of end-functionalized polymers: an NMR approach via combination of one-dimensional and two-dimensional techniques. Chin J Polym Sci 35(5):681–692

36. Bharti SK, Roy R (2012) Quantitative 1H NMR spectroscopy. Analyt Chem 35:5–26

37. Izunobi JU, Higginbotham CL (2011) Polymer molecular weight analysis by ^{1}H NMR spectroscopy. J Chem Ed 88(8):1098–1104

38. Ziaee F (2013) Application of nuclear magnetic resonance in polymers (In Persian). Iran Polymer and Petrochemical Institute, Tehran

39. Stuart BH (2004) Infrared spectroscopy: fundamentals and applications. Wiley, New Jersey

40. Zhang P, He J, Zhou X (2008) An FTIR standard addition method for quantification of bound styrene in its copolymers. Polym Test 27(2):153–157

41. Deygen Irina M, Kudryashova EV (2016) New versatile approach for analysis of PEG content in conjugates and complexes with biomacromolecules based on FTIR spectroscopy. Colloids Surf B 141(1):36–43

42. Bakhshi H, Zohuriaan-Mehr MJ, Bouhendi H, Kabiri K (2009) Spectral and chemical determination of copolymer composition of poly (butyl acrylate-co-glycidyl methacrylate) from emulsion polymerization. Polym Test 28(7):730–736

43. Mamun A, Rahman SM, Roland S, Mahmood R (2018) Impact of molecular weight on the thermal stability and the miscibility of poly (ε-caprolactone)/polystyrene binary blends. J Polym Environm 26(8):3511–3519